Scientia Iranica F (2016) 23(6), 3099–3114

Sharif University of Technology
Scientia Iranica
Transactions F: Nanotechnology
www.scientiairanica.com

Nonlocal nonlinear first-order shear deformable beam model for post-buckling analysis of magneto-electro-thermo-elastic nanobeams

R. Ansari[a] and R. Gholami[b,*]

a. *Department of Mechanical Engineering, University of Guilan, Rasht, P.O. Box 41635-3756, Iran.*
b. *Department of Mechanical Engineering, Lahijan Branch, Islamic Azad University, Lahijan, P.O. Box 1616, Iran.*

Received 22 August 2015; received in revised form 6 April 2016; accepted 26 September 2016

KEYWORDS
First-order shear deformable nanobeam;
Magneto-electro-thermo-elastic materials;
Post-buckling;
Nonlocal elasticity theory;
Small-scale effect.

Abstract. In this study, the size-dependent post-buckling behavior of Magneto-Electro-Thermo-Elastic (METE) nanobeams with different edge supports is investigated. Based on the nonlocal first-order shear deformation beam theory and considering the von Kármán hypothesis, a size-dependent nonlinear METE nanobeam model is developed, in which the effects of small-scale parameter and thermo-electro-magnetic-mechanical loadings are incorporated. A numerical solution procedure based on the Generalized Differential Quadrature (GDQ) and pseudo arc-length continuation methods is utilized to describe the size-dependent post-buckling behavior of METE nanobeams under various boundary conditions. The effects of different parameters such as nonlocal parameter, external electric voltage, external magnetic potential, and temperature rise on the post-buckling path of METE nanobeams are explored. The results indicate that increasing the non-dimensional nonlocal parameter, imposed positive voltage, negative magnetic potential, and temperature rise decreases the critical buckling load and post-buckling load-carrying capacity of METE nanobeams, while an increase in the negative voltage and positive magnetic potential leads to a considerable increase of critical buckling load as well as post-buckling strength of the METE nanobeams.

1. Introduction

Due to their inherent coupling of field quantities, the Magnet-Electro-Thermo-Elastic (METE) materials have attracted much attention recently [1-5]. The superior properties of METE structures enable them to be used in a wide range of engineering applications such as transducers, actuators, vibration control devices, resonators, robotics, and high-density information storage devices [6-11]. Also, due to the rapid advancement in modern nanoscience, nanotechnology, and Nano- and Micro-Electro-Mechanical Systems (NEMS and MEMS), the development of the new class of smart or intelligent nanostructures made of METE materials has received considerable attention. These nanostructures have the capability to be used in many novel nanoscale devises such as sensors and NEMS devices [12,13]. Due to the dependence of mechanical characteristics of nanostructures on the size effects, which has been proven in the experimental tests and molecular dynamics simulations [14-17], considering the size effects in the continuum models is necessary.

In recent years, the size-dependent mechanical behaviors of nanostructures, such as nanobeams, nanoplates, and nanoshells, have attracted the attention of researchers [18-27]. For instance, the Eringen's nonlocal elasticity theory [28-30] has been

*. *Corresponding author. Tel./Fax: +98 1342222906*
E-mail address: gholami_@liau.ac.ir (R. Gholami)

extended to the METE material to take the size effects into account [31-34]. Using a nonlocal Timoshenko beam model, the thermoelectric-mechanical vibration of piezoelectric nanobeams was examined by Ke and Wang [35]. Further, considering the influence of magnetic potential, Ke and Wang [36] developed a nonlocal METE beam model to investigate the effects of important parameters such as the nonlocal parameter, temperature rise, and external electric and magnetic potentials on the free vibration of METE Timoshenko nanobeams with various boundary conditions. According to the nonlocal theory and Kirchhoff plate theory, Ke et al. [37] analyzed the free vibration of size-dependent METE nanoplates with simply-supported edge conditions. Also, based on the nonlocal Mindlin plate theory, the free vibration of piezoelectric rectangular nanoplates with various boundary conditions under the thermo-electro-mechanical loading was studied by Ke et al. [38]. A nonlocal magneto-electro-elastic Mindlin nanoplate model was proposed by Li et al. [39] for the analysis of size-dependent buckling and free vibration of magneto-electro-elastic nanoplates. Recently, Ke et al. [40] developed a nonlocal METE cylindrical nanoshell model based on the Love's shell and Eringen's nonlocal elasticity theories. This model includes the influences of the small-scale parameter and magneto-electro-thermal loadings. Moreover, a few studies have been performed to investigate the surface effect on the mechanical characteristics of piezoelectric nanostructures [41-44].

Although several nonlocal beam, plate, and shell models have been developed to examine the free vibration characteristics of METE nanostructures, the buckling behavior of nanobeams with different boundary conditions under the magneto-electro-thermo-mechanical loading has not been considered. Moreover, the investigations have been done by employing the linear METE models and the geometrical nonlinearities in the METE nanosystems have been absolutely excluded. When the METE nanostructures are subjected to a large amplitude vibration or a buckling instability, these linear size-dependent METE models are not capable of predicting the mechanical characteristics of METE nanostructures. Therefore, the geometric nonlinearities must be considered.

To the authors' best knowledge, the size-dependent post-buckling analysis of the METE nanobeams has not been reported so far. Hence, in this study, it is attempted to develop a size-dependent nonlinear first-order shear deformable nanobeam model to examine the post-buckling characteristics of METE nanobeams with different edge supports. By means of the Eringen's nonlocal elasticity theory, first-order shear deformation beam theory, and von Kármán hypothesis, the nonlinear governing equations and corresponding boundary conditions are obtained. The developed beam model contains the effects of small-scale parameter, thermo-electro-magnetic-mechanical loadings, and transverse shear deformation. Then, the Generalized Differential Quadrature (GDQ) method is utilized to discretize the nonlinear governing equations, which are then solved using the pseudo arc-length continuation method to obtain the post-buckling path of the METE nanobeams under various edge supports. Finally, numerical results in the graphical forms are provided to investigate the effects of various parameters such as the nonlocal parameter, external electric voltage, external magnetic potential, and temperature rise on the post-buckling path of METE nanobeams.

This paper is organized as follows; in Section 2, the nonlocal elasticity theory for the METE materials is introduced and the mathematical modeling of the METE nanobeam is presented. By considering the appropriate non-dimensional parameters, the non-dimensional form of size-dependent governing equations is given in Section 3. In Section 4, the post-buckling problem of the METE nanobeams is numerically solved using the GDQ method and pseudo arc-length continuation algorithm. Results and discussion are presented in Section 5 and concluding remarks are given in Section 6.

2. Problem formulation

2.1. A brief overview of the nonlocal elasticity theory for the METE materials

According to the Eringen's nonlocal elasticity theory [28-30] and considering this hypothesis that the stress at reference point in a continuum body is a function of the strain field at all points in the body, the basic relations for a homogeneous and METE solid are written mathematically as:

$$\sigma_{ij} = \int_V \lambda(|x-x'|,\mu)[c_{ijkl}\varepsilon_{kl}(x') - e_{mij}E_m(x') - q_{nij}H_n(x') - \beta_{ij}\Delta T]dV(x'), \quad \forall\ x \in V, \tag{1a}$$

$$D_i = \int_V \lambda(|x-x'|,\mu)[e_{ikl}\varepsilon_{kl}(x') + s_{im}E_m(x') + d_{in}H_n(x') + p_i\Delta T]dV(x'), \quad \forall\ x \in V, \tag{1b}$$

$$B_i = \int_V \lambda(|x-x'|,\mu)[q_{ikl}\varepsilon_{kl}(x') + d_{im}E_m(x') + \mu_{in}H_n(x') + \lambda_i\Delta T]dV(x'), \quad \forall\ x \in V, \tag{1c}$$

where σ_{ij}, D_i, and B_i represent the components of stress, electric displacement, and magnetic induction,

respectively; and ε_{ij}, E_i, and H_i denote the components of the strain, electric field, and magnetic field, respectively. Moreover, c_{ijkl}, e_{mij}, s_{im}, q_{nij}, d_{ij}, s_{ij}, p_i, and λ_i are, respectively, the elastic, piezoelectric, dielectric, piezomagnetic, magnetoelectric, magnetic, pyroelectric, and pyromagnetic constants; and β_{ij} and ΔT denote the thermal moduli and temperature change, respectively. Also, $\lambda, |x - x'|$, and $\mu = e_0 a/l$ denote the nonlocal modulus, Euclidean distance, and scale coefficient, respectively; and e_0, a, and l are, respectively, a non-dimensional material property, internal characteristic length, and external characteristic length of the nanostructures. The parameter $e_0 a$ denotes the nonlocal parameter incorporating the small-scale effect into the response of the nano-scale structures, which is obtained from molecular dynamics, experimental data, or comparison of calculations based on lattice dynamics, to calibrate the nonlocal continuum models.

According to Eringen's theory [29], the spatial integral constitutive relation (Eqs. (1)) can be expressed as the equivalent differential constitutive equations as:

$$\sigma_{ij} - (e_0 a)^2 \nabla^2 \sigma_{ij} = c_{ijkl}\varepsilon_{kl} - e_{mij}E_m - q_{nij}H_n - \beta_{ij}\Delta T, \tag{2a}$$

$$D_i - (e_0 a)^2 \nabla^2 D_i = e_{ikl}\varepsilon_{kl} + s_{im}E_m + d_{in}H_n + p_i \Delta T, \tag{2b}$$

$$B_i - (e_0 a)^2 \nabla^2 B_i = q_{ikl}\varepsilon_{kl} + d_{im}E_m + \mu_{in}H_n + \lambda_i \Delta T, \tag{2c}$$

in which ∇^2 represents the Laplace operator.

Considering the quasi-static approximation, which neglects the electric and magnetic charge densities, the electric field vector and magnetic intensity vector can be respectively obtained by means of the Maxwell theory as follows [39]:

$$\mathbf{E} = -\nabla \Phi, \tag{3a}$$

$$\mathbf{H} = -\nabla \Psi, \tag{3b}$$

in which Φ and Ψ denote the scalar electric and magnetic potentials, respectively.

2.2. Governing equations and corresponding boundary conditions

The considered system is an METE nanobeam of length, L, thickness, h, cross sectional area A, and moment of inertia of the cross section, I, as depicted in Figure 1. The METE nanobeam is subjected to an electric potential, $\Phi(x, z)$, a magnetic potential, $\Psi(x, z)$, a uniform temperature rise, ΔT, and a compressive axial load, N_x^0. Based upon the first-order shear deformation beam theory, the displacements of an arbitrary point in the METE nanobeam along the axial direction, x, and lateral direction, z, respectively, defined by $u_x(x, z)$ and $u_z(x, z)$, are given by:

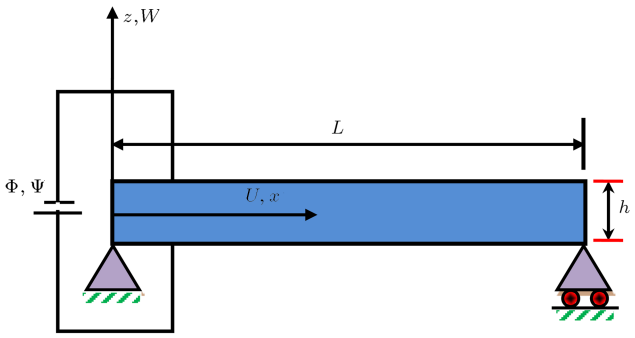

Figure 1. Schematic view of an METE nanobeam.

$$u_x(x, z) = U(x) + z\Theta_x(x), \qquad u_z(x, z) = W(x), \tag{4}$$

where U is the axial displacement of the center of sections; W stands for the lateral deflection of the METE nanobeam; and Θ_x denotes the rotation of beam cross section.

Assuming that the METE nanobeam is subjected to small slopes after deflection, the von Kármán hypothesis can be utilized to express the nonlinear strain-displacement relations as follows:

$$\varepsilon_{xx} = \frac{du_x}{dx} + \frac{1}{2}\left(\frac{dW}{dx}\right)^2 = \frac{dU}{dx} + z\frac{d\Theta_x}{dx} + \frac{1}{2}\left(\frac{dW}{dx}\right)^2,$$

$$\gamma_{xz} = \left(\Theta_x + \frac{dW}{dx}\right). \tag{5}$$

Moreover, the electric potential and magnetic potential are, respectively, considered as [36]:

$$\Phi = -\cos(\beta z)\phi_E(x) + \frac{2z}{h}V_E, \tag{6a}$$

$$\Psi = -\cos(\beta z)\psi_H(x) + \frac{2z}{h}\Omega_H, \tag{6b}$$

in which $\beta = \pi/h$; V_E and Ω_H denote the initial external electric and magnetic potentials, respectively; and $\phi_E(x)$ and $\psi_H(x)$ represent the variations of the electric and magnetic potentials in the x-direction, respectively.

Substituting Eqs. (6a) and (6b) into Eqs. (3a) and (3b), the non-zero components of electric fields (E_x, E_z) and magnetic fields (H_x, H_z) can be easily derived as follows:

$$E_x = -\frac{d\Phi}{dx} = \cos(\beta z)\frac{d\phi_E}{dx},$$

$$E_z = -\frac{d\Phi}{dz} = -\beta \sin(\beta z)\phi_E - \frac{2V_E}{h}, \tag{7a}$$

$$H_x = -\frac{d\Psi}{dx} = \cos(\beta z)\frac{d\psi_H}{dx},$$

$$H_z = -\frac{d\Psi}{dz} = -\beta \sin(\beta z)\psi_H - \frac{2\Omega_H}{h}. \tag{7b}$$

The strain energy Π_s of METE nanobeams can be obtained as:

$$\Pi_s = \frac{1}{2}\int_0^L \int_A (\sigma_{xx}\varepsilon_{xx} + \sigma_{xz}\gamma_{xz} - D_x E_x - D_z E_z - B_x H_x - B_z H_z) dA dx. \tag{8}$$

Inserting Eqs. (5) and (7) into Eq. (8) yields:

$$\begin{aligned}\Pi_s =& \frac{1}{2}\int_0^L \left\{ N_x \left[\frac{\partial U}{\partial x} + \frac{1}{2}\left(\frac{dW}{dx}\right)^2 \right] + M_x \frac{d\Theta_x}{dx} + Q_x \left(\frac{dW}{dx} + \Theta_x \right) \right\} dx \\ &+ \frac{1}{2}\int_0^L \int_A \left(-D_x \cos(\beta z)\frac{d\phi_E}{dx} + D_z \left(\beta \sin(\beta z)\phi_E + \frac{2V_E}{h} \right) \right) dA dx \\ &+ \frac{1}{2}\int_0^L \int_A \left(-B_x \cos(\beta z)\frac{d\psi_H}{dx} + B_z \left(\beta \sin(\beta z)\psi_H + \frac{2\Omega_H}{h} \right) \right) dA dx, \end{aligned} \tag{9}$$

where the normal resultant force, N_x, transverse shear force, Q_x, and bending moment, M_x, present in Eq. (9), can be obtained by:

$$N_x = \int_A \sigma_{xx} dA, \qquad M_x = \int_A \sigma_{xx} z dA,$$

$$Q_x = \kappa_s \int_A \sigma_{xz} dA, \tag{10}$$

in which $\kappa_s = 5/6$ is the shear correction factor. Moreover, the work done by applied external axial load, N_x^0, can be calculated from:

$$\Pi_{ex} = \frac{1}{2}\int_0^L N_x^0 \left(\frac{dW}{dx}\right)^2 dx. \tag{11}$$

By means of the principle of minimum total potential energy and fundamental lemma of the calculus of variation ($\delta\Pi_s - \delta\Pi_{ex} = 0$; δ is the variational operator), the nonlinear governing equations of an METE beam corresponding to the classical Timoshenko beam theory are derived as:

$$\frac{dN_x}{dx} = 0, \tag{12a}$$

$$\frac{d}{dx}\left(N_x \frac{dW}{dx} \right) + \frac{dQ_x}{dx} + N_x^0 \frac{d^2 W}{dx^2} = 0, \tag{12b}$$

$$\frac{dM_x}{dx} - Q_x = 0, \tag{12c}$$

$$\int_A \left(\cos(\beta z)\frac{dD_x}{dx} + \beta \sin(\beta z) D_z \right) dA = 0, \tag{12d}$$

$$\int_A \left(\cos(\beta z)\frac{dB_x}{dx} + \beta \sin(\beta z) B_z \right) dA = 0. \tag{12e}$$

Also, the mathematical expressions of associated boundary conditions at beam ends ($x = 0, L$) are derived:

$$\delta U = 0 \quad \text{or} \quad N_x = 0, \tag{13a}$$

$$\delta W = 0 \quad \text{or} \quad (N_x + N_x^0)\frac{dW}{dx} + Q_x = 0, \tag{13b}$$

$$\delta \Theta_x = 0 \quad \text{or} \quad M_x = 0, \tag{13c}$$

$$\delta \phi_E = 0 \quad \text{or} \quad \int_A \cos(\beta z) D_x dA = 0, \tag{13d}$$

$$\delta \psi_H = 0 \quad \text{or} \quad \int_A \cos(\beta z) B_x dA = 0. \tag{13e}$$

Now, to take the small-scale effect into account, the Eringen's nonlocal elasticity theory is used. According to Eqs. (2), (5), and (7), the nonlocal constitutive relations for the METE beams under the plane stress condition can be obtained as:

$$\begin{aligned}\sigma_{xx} - (e_0 a)^2 \frac{d^2 \sigma_{xx}}{dx^2} =& \tilde{c}_{11}\left[\frac{dU}{dx} + z\frac{d\Theta_x}{dx} + \frac{1}{2}\left(\frac{dW}{dx}\right)^2 \right] \\ &+ \tilde{e}_{31}\left(\beta \sin(\beta z)\phi_E + \frac{2V_E}{h} \right) \\ &+ \tilde{q}_{31}\left(\beta \sin(\beta z)\psi_H + \frac{2\Omega_H}{h} \right) - \tilde{\beta}_1 \Delta T, \end{aligned} \tag{14a}$$

$$\sigma_{xz} - (e_0a)^2\frac{d^2\sigma_{xz}}{dx^2} = \tilde{c}_{44}\left(\Theta_x + \frac{dW}{dx}\right) - \tilde{e}_{15}\cos(\beta z)\frac{d\phi_E}{dx} - \tilde{q}_{15}\cos(\beta z)\frac{d\psi_H}{dx}, \quad (14b)$$

$$D_x - (e_0a)^2\frac{d^2D_x}{dx^2} = \tilde{e}_{15}\left(\Theta_x + \frac{dW}{dx}\right) + \tilde{s}_{11}\cos(\beta z)\frac{d\phi_E}{dx} + \tilde{d}_{11}\cos(\beta z)\frac{d\psi_H}{dx}, \quad (14c)$$

$$D_z - (e_0a)^2\frac{d^2D_z}{dx^2} = \tilde{e}_{31}\left[\frac{dU}{dx} + z\frac{d\Theta_x}{dx} + \frac{1}{2}\left(\frac{dW}{dx}\right)^2\right] - \tilde{s}_{33}\left(\beta\sin(\beta z)\phi_E + \frac{2V_E}{h}\right) - \tilde{d}_{33}\left(\beta\sin(\beta z)\psi_H + \frac{2\Omega_H}{h}\right) + \tilde{p}_3\Delta T, \quad (14d)$$

$$B_x - (e_0a)^2\frac{d^2B_x}{dx^2} = \tilde{q}_{15}\left(\Theta_x + \frac{dW}{dx}\right) + \tilde{d}_{11}\cos(\beta z)\frac{d\phi_E}{dx} + \tilde{\mu}_{11}\cos(\beta z)\frac{d\psi_H}{dx}, \quad (14e)$$

$$B_z - (e_0a)^2\frac{d^2B_z}{dx^2} = \tilde{q}_{31}\left[\frac{dU}{dx} + z\frac{d\Theta_x}{dx} + \frac{1}{2}\left(\frac{dW}{dx}\right)^2\right] - \tilde{d}_{33}\left(\beta\sin(\beta z)\phi_E + \frac{2V_E}{h}\right) - \tilde{\mu}_{33}\left(\beta\sin(\beta z)\psi_H + \frac{2\Omega_H}{h}\right) + \tilde{\lambda}_3\Delta T, \quad (14f)$$

where $\tilde{c}_{ij}$, $\tilde{e}_{ij}$, $\tilde{s}_{ij}$, $\tilde{q}_{ij}$, $\tilde{d}_{ij}$, $\tilde{\mu}_{ij}$, $\tilde{\beta}_i$, $\tilde{p}_i$, and $\tilde{\lambda}_i$ denote the reduced elastic, piezoelectric, dielectric constants, piezomagnetic, magnetoelectric, magnetic, thermal moduli, pyroelectric, and pyromagnetic constants for the METE nanobeam under the plane stress condition, respectively. These constants can be obtained as:

$$\tilde{c}_{11} = c_{11} - \frac{c_{13}^2}{c_{33}}, \quad \tilde{c}_{44} = c_{44},$$
$$\tilde{e}_{31} = e_{31} - \frac{c_{13}e_{33}}{c_{33}}, \quad \tilde{e}_{15} = e_{15},$$
$$\tilde{q}_{31} = q_{31} - \frac{c_{13}q_{33}}{c_{33}}, \quad \tilde{s}_{11} = s_{11},$$
$$\tilde{s}_{33} = s_{33} + \frac{e_{33}^2}{c_{33}}, \quad \tilde{d}_{11} = d_{11},$$
$$\tilde{d}_{33} = d_{33} + \frac{q_{33}e_{33}}{c_{33}}, \quad \tilde{\mu}_{11} = \mu_{11},$$
$$\tilde{\mu}_{33} = \mu_{33} + \frac{q_{33}^2}{c_{33}}, \quad \tilde{q}_{15} = q_{15},$$
$$\tilde{\beta}_1 = \beta_1 - \frac{c_{13}\beta_3}{c_{33}}, \quad \tilde{p}_3 = p_3 + \frac{\beta_3 e_{33}}{c_{33}},$$
$$\tilde{\lambda}_3 = \lambda_3 + \frac{\beta_3 q_{33}}{c_{33}}. \quad (15)$$

By use of Eq. (14), the following relations associated with the nonlocal form of N_x, Q_x, M_x, D_x, D_z, B_x, and B_z are obtained as:

$$N_x - (e_0a)^2\frac{d^2N_x}{dx^2} = A_{11}\left[\frac{dU}{dx} + \frac{1}{2}\left(\frac{dW}{dx}\right)^2\right] + N_E + N_H + N_T, \quad (16a)$$

$$M_x - (e_0a)^2\frac{d^2M_x}{dx^2} = D_{11}\frac{d\Theta_x}{dx} + E_{31}\phi_E + Q_{31}\psi_H, \quad (16b)$$

$$Q_x - (e_0a)^2\frac{d^2Q_x}{dx^2} = k_sA_{44}\left(\Theta_x + \frac{dW}{dx}\right) - \kappa_sE_{15}\frac{d\phi_E}{dx} - \kappa_sQ_{15}\frac{d\psi_H}{dx}, \quad (16c)$$

$$\int_A \left\{D_x - (e_0a)^2\frac{d^2D_x}{dx^2}\right\}\cos(\beta z)dA = E_{15}\left(\Theta_x + \frac{dW}{dx}\right) + X_{11}\frac{d\phi_E}{dx} + Y_{11}\frac{d\psi_H}{dx}, \quad (16d)$$

$$\int_A \left\{D_z - (e_0a)^2\frac{d^2D_z}{dx^2}\right\}\beta\sin(\beta z)dA = E_{31}\frac{d\Theta_x}{dx} - X_{33}\phi_E - Y_{33}\psi_H, \quad (16e)$$

$$\int_A \left\{ B_x - (e_0 a)^2 \frac{d^2 B_x}{dx^2} \right\} \cos(\beta z) dA = Q_{15} \left(\Theta_x + \frac{dW}{dx} \right) + Y_{11} \frac{d\phi_E}{dx} + T_{11} \frac{d\psi_H}{dx}, \quad (16f)$$

$$\int_A \left\{ B_z - (e_0 a)^2 \frac{d^2 B_z}{dx^2} \right\} \beta \sin(\beta z) dA = Q_{31} \frac{d\Theta_x}{dx} - Y_{33} \phi_E - T_{33} \psi_H. \quad (16g)$$

The constant coefficients present in Eq. (6) are defined as:

$$N_E = \frac{2\tilde{e}_{31} V_E A}{h}, \qquad N_H = \frac{2\tilde{q}_{31} \Omega_H A}{h},$$

$$N_T = -\tilde{\beta}_1 A \Delta T, \quad (17a)$$

$$A_{11} = \tilde{c}_{11} A, \qquad A_{44} = \tilde{c}_{44} A, \qquad D_{11} = \tilde{c}_{11} I, \quad (17b)$$

$$E_{31} = \int_A \tilde{e}_{31} \beta \sin(\beta z) z dA,$$

$$Q_{31} = \int_A \tilde{q}_{31} \beta \sin(\beta z) z dA, \quad (17c)$$

$$E_{15} = \int_A \tilde{e}_{15} \cos(\beta z) dA,$$

$$Q_{15} = \int_A \tilde{q}_{15} \cos(\beta z) dA, \quad (17d)$$

$$X_{11} = \int_A \tilde{s}_{11} \cos^2(\beta z) dA,$$

$$Y_{11} = \int_A \tilde{d}_{11} \cos^2(\beta z) dA,$$

$$T_{11} = \int_A \tilde{\mu}_{11} \cos^2(\beta z) dA, \quad (17e)$$

$$X_{33} = \int_A \tilde{s}_{33} [\beta \sin(\beta z)]^2 dA,$$

$$Y_{33} = \int_A \tilde{d}_{33} [\beta \sin(\beta z)]^2 dA,$$

$$T_{33} = \int_A \tilde{\mu}_{33} [\beta \sin(\beta z)]^2 dA. \quad (17f)$$

By substituting Eqs. (16a)-(16c) into Eqs. (12a)-(12c), the nonlocal normal resultant force, N_x, bending moment, M_x, and transverse shear force, Q_x, can be explicitly expressed in the following form:

$$N_x = A_{11} \left[\frac{dU}{dx} + \frac{1}{2} \left(\frac{dW}{dx} \right)^2 \right] + N_E + N_H + N_T, \quad (18a)$$

$$M_x = D_{11} \frac{d\Theta_x}{dx} + E_{31} \phi_E + Q_{31} \psi_H - (e_0 a)^2 \frac{d}{dx} \left([N_x + N_x^0] \frac{dW}{dx} \right), \quad (18b)$$

$$Q_x = k_s A_{44} \left(\Theta_x + \frac{dW}{dx} \right) - \kappa_s E_{15} \frac{d\phi_E}{dx} - \kappa_s Q_{15} \frac{d\psi_H}{dx} - (e_0 a)^2 \frac{d^2}{dx^2} \left([N_x + N_x^0] \frac{dW}{dx} \right). \quad (18c)$$

It should be noted that the nonlocal forms of D_x, D_z, B_x, and B_z cannot be explicitly obtained by substituting Eqs. (16d) and (16e) into Eqs. (12d)-(12g). However, the nonlocal form of governing equilibrium equations for the METE nanobeams can be expressed in terms of U, W, Θ_x, ϕ_E, and ψ_H as follows:

$$A_{11} \left(\frac{d^2 U}{dx^2} + \frac{dW}{\partial x} \frac{d^2 W}{dx^2} \right) = 0, \quad (19a)$$

$$k_s A_{44} \left(\frac{d\Theta_x}{dx} + \frac{d^2 W}{dx^2} \right) + \left(N_x^0 + N_E + N_H + N_T \right) \left(\frac{d^2 W}{dx^2} - (e_0 a)^2 \frac{d^4 W}{dx^4} \right) - \kappa_s \left(E_{15} \frac{d^2 \phi_E}{dx^2} + Q_{15} \frac{d^2 \psi_H}{dx^2} \right) + Z_1 - (e_0 a)^2 Z_2 = 0, \quad (19b)$$

$$D_{11} \frac{d^2 \Theta_x}{dx^2} - k_s A_{44} \left(\Theta_x + \frac{dW}{dx} \right) + (E_{31} + \kappa_s E_{15}) \frac{d\phi_E}{dx} + (Q_{31} + \kappa_s Q_{15}) \frac{d\phi_E}{dx} = 0, \quad (19c)$$

$$E_{31} \frac{d\Theta_x}{dx} + E_{15} \left(\frac{d^2 W}{dx^2} + \frac{d\Theta_x}{dx} \right) + X_{11} \frac{d^2 \phi_E}{dx^2} + Y_{11} \frac{d^2 \psi_H}{dx^2} - X_{33} \phi_E - Y_{33} \psi_H = 0, \quad (19d)$$

$$Q_{31}\frac{d\Theta_x}{dx}+Q_{15}\left(\frac{d^2W}{dx^2}+\frac{d\Theta_x}{dx}\right)+Y_{11}\frac{d^2\phi_E}{dx^2}+T_{11}\frac{d^2\psi_H}{dx^2}-Y_{33}\phi_E-T_{33}\psi_H=0, \tag{19e}$$

where:

$$Z_1=A_{11}\left(\frac{d^2U}{dx^2}\frac{dW}{dx}+\frac{dU}{dx}\frac{d^2W}{dx^2}+\frac{3}{2}\left(\frac{dW}{dx}\right)^2\frac{d^2W}{dx^2}\right), \tag{20a}$$

$$Z_2=A_{11}\left(\frac{d^4U}{dx^4}\frac{dW}{dx}+3\frac{d^3U}{dx^3}\frac{d^2W}{dx^2}+3\frac{d^2U}{dx^2}\frac{d^3W}{dx^3}+\frac{dU}{dx}\frac{d^4W}{dx^4}\right)+A_{11}\left[3\left(\frac{d^2W}{dx^2}\right)^2+9\frac{dW}{dx}\frac{d^2W}{dx^2}\frac{d^3W}{dx^3}+\frac{3}{2}\left(\frac{dW}{dx}\right)^2\frac{d^4W}{dx^4}\right]. \tag{20b}$$

Eqs. (19a)-(19e) represent the size-dependent nonlinear equilibrium equations of a first-order shear deformable METE nanobeam modeled on the basis of the Eringen's nonlocal elasticity theory.

3. Non-dimensional form of size-dependent nonlinear governing equations

Introducing the following non-dimensional parameters:

$$\xi=\frac{x}{L},\qquad (u,w)=\frac{(U,W)}{h},\qquad \theta_x=\Theta_x,$$

$$\phi=\frac{\phi_E}{\phi_0},\qquad \psi=\frac{\psi_H}{\psi_0},\qquad \phi_0=\sqrt{A_{11}/X_{33}},$$

$$\psi_0=\sqrt{A_{11}/T_{33}},\qquad \epsilon=\frac{e_0a}{L},\qquad \eta=\frac{L}{h},$$

$$\left(\bar{N}_x^0,\bar{N}_T,\bar{N}_E,\bar{N}_H\right)=\left(\frac{N_x^0}{A_{11}},\frac{N_T}{A_{11}},\frac{N_E}{A_{11}},\frac{N_H}{A_{11}}\right),$$

$$\left(\bar{A}_{11},\bar{A}_{44},\bar{D}_{11}\right)=\left(\frac{A_{11}}{A_{11}},\frac{A_{44}}{A_{11}},\frac{D_{11}}{A_{11}h^2}\right),$$

$$\left(\bar{E}_{15},\bar{E}_{31}\right)=\left(\frac{E_{15}\phi_0}{A_{11}h},\frac{E_{31}\phi_0}{A_{11}h}\right),$$

$$\left(\bar{Q}_{15},\bar{Q}_{31}\right)=\left(\frac{Q_{15}\psi_0}{A_{11}h},\frac{Q_{31}\psi_0}{A_{11}h}\right),$$

$$\left(\bar{X}_{11},\bar{X}_{33}\right)=\left(\frac{X_{11}\phi_0^2}{A_{11}h^2},\frac{X_{33}\phi_0^2}{A_{11}}\right),$$

$$\left(\bar{T}_{11},\bar{T}_{33}\right)=\left(\frac{T_{11}\psi_0^2}{A_{11}h^2},\frac{T_{33}\psi_0^2}{A_{11}}\right),$$

$$\left(\bar{Y}_{11},\bar{Y}_{33}\right)=\left(\frac{Y_{11}\phi_0\psi_0}{A_{11}h^2},\frac{Y_{33}\phi_0\psi_0}{A_{11}}\right), \tag{21}$$

the non-dimensional equilibrium equations (Eqs. (19a)-(19e)) can be expressed as:

$$\bar{A}_{11}\left(\frac{d^2u}{d\xi^2}+\frac{1}{\eta}\frac{dw}{d\xi}\frac{d^2w}{d\xi^2}\right)=0, \tag{22a}$$

$$k_s\bar{A}_{44}\left(\frac{d^2w}{d\xi^2}+\eta\frac{d\theta_x}{d\xi}\right)+\left(\bar{N}_x^0+\bar{N}_T+\bar{N}_E+\bar{N}_H\right)\left(\frac{d^2w}{d\xi^2}-\epsilon^2\frac{d^4w}{d\xi^4}\right)-k_s\bar{E}_{15}\frac{d^2\bar{\phi}_E}{d\xi^2}-k_s\bar{Q}_{15}\frac{d^2\bar{\psi}_H}{d\xi^2}+\bar{Z}_1-\epsilon^2\bar{Z}_2=0, \tag{22b}$$

$$\bar{D}_{11}\frac{d^2\theta_x}{d\xi^2}-k_s\bar{A}_{44}\eta\left(\frac{dw}{d\xi}+\eta\theta_x\right)+\eta\left(\bar{E}_{31}+\kappa_s\bar{E}_{15}\right)\frac{d\phi}{d\xi}+\eta\left(\bar{Q}_{31}+\kappa_s\bar{Q}_{15}\right)\frac{d\psi}{d\xi}=0, \tag{22c}$$

$$\bar{E}_{31}\eta\frac{d\theta_x}{d\xi}+\bar{E}_{15}\left(\frac{d^2w}{d\xi^2}+\eta\frac{d\theta_x}{d\xi}\right)+\bar{X}_{11}\frac{d^2\phi}{d\xi^2}+\bar{Y}_{11}\frac{d^2\psi}{d\xi^2}-\bar{X}_{33}\eta^2\phi-\bar{Y}_{33}\eta^2\psi=0, \tag{22d}$$

$$\bar{Q}_{31}\eta\frac{d\theta_x}{d\xi}+Q_{15}\left(\frac{d^2w}{d\xi^2}+\eta\frac{d\theta_x}{d\xi}\right)+\bar{Y}_{11}\frac{d^2\phi}{d\xi^2}+\bar{T}_{11}\frac{d^2\psi}{d\xi^2}-\bar{Y}_{33}\eta^2\phi-\bar{T}_{33}\eta^2\psi=0, \tag{22e}$$

in which the nonlinear terms, $\bar{Z}_1$ and $\bar{Z}_2$, are defined as:

$$\bar{Z}_1=\frac{\bar{A}_{11}}{\eta}\left(\frac{d^2u}{d\xi^2}\frac{dw}{d\xi}+\frac{3}{2\eta}\left(\frac{dw}{d\xi}\right)^2\frac{d^2w}{d\xi^2}+\frac{du}{d\xi}\frac{d^2w}{d\xi^2}\right),$$

$$\bar{Z}_2 = \frac{\bar{A}_{11}}{\eta}\left(\frac{d^4u}{d\xi^4}\frac{dw}{d\xi}+3\frac{d^3u}{d\xi^3}\frac{d^2w}{d\xi^2}+3\frac{d^2u}{d\xi^2}\frac{d^3w}{d\xi^3}+\frac{du}{d\xi}\frac{d^4w}{d\xi^4}\right) + \frac{\bar{A}_{11}}{\eta^2}\left[3\left(\frac{d^2w}{d\xi^2}\right)^3+9\frac{dw}{d\xi}\frac{d^2w}{d\xi^2}\frac{d^3w}{d\xi^3}+\frac{3}{2}\left(\frac{dw}{d\xi}\right)^2\frac{d^4w}{d\xi^4}\right]. \quad (23)$$

Assuming the electric potential and magnetic potential to be zero at the ends of the METE nanobeam, the mathematical expressions of edge supports can be written in the non-dimensional forms as:

$$u = w = \theta_x = \phi = \psi = 0 \quad \text{at} \quad \xi = 0,$$
$$\bar{N}_x = w = \theta_x = \phi = \psi = 0 \quad \text{at} \quad \xi = 1, \quad (24)$$

for a Clamped-Clamped (C-C) end condition:

$$u = w = \bar{M}_x = \phi = \psi = 0 \quad \text{at} \quad \xi = 0,$$
$$\bar{N}_x = w = \bar{M}_x = \phi = \psi = 0 \quad \text{at} \quad \xi = 1, \quad (25)$$

for a Simply Supported-Simply Supported (SS-SS) end condition, and:

$$u = w = \theta_x = \phi = \psi = 0 \quad \text{at} \quad \xi = 0,$$
$$\bar{N}_x = w = \bar{M}_x = \phi = \psi = 0 \quad \text{at} \quad \xi = 1, \quad (26)$$

for a Clamped-Simply Supported (C-SS) end condition, in which:

$$\bar{N}_x = \bar{A}_{11}\left[\frac{du}{d\xi}+\frac{1}{2\eta}\left(\frac{dw}{d\xi}\right)^2\right]+\bar{N}_x^0+\bar{N}_E+\bar{N}_H+\bar{N}_T,$$
$$\bar{M}_x = \bar{D}_{11}\frac{d\theta_x}{d\xi}+\eta\bar{E}_{31}\phi+\eta\bar{Q}_{31}\psi - \epsilon^2\eta\left(\bar{N}_x^0+\bar{N}_E+\bar{N}_H+\bar{N}_T\right)\frac{d^2w}{d\xi^2} - \epsilon^2\bar{A}_{11}\frac{d}{d\xi}\left(\left[\frac{du}{d\xi}+\frac{1}{2\eta}\left(\frac{dw}{d\xi}\right)^2\right]\frac{dw}{d\xi}\right). \quad (27)$$

It should be remarked that in the applications of METE devices such as sensors and actuators, two kinds of boundary conditions for the electric and magnetic potential can be considered. One of them is open circuit with the assumption of:

$$\int_A \cos(\beta z)D_x dA = \int_A \cos(\beta z)B_x dA = 0.$$

This type of boundary conditions is for the sensor situation [45]. Another type of boundary condition is short circuit with the assumption of $\phi = \psi = 0$, which is for the actuator case [45]. In the present study, the short circuit has been considered and it is assumed that $\phi = \psi = 0$.

4. Numerical solution

To solve the post-buckling problem of METE nanobeams subjected to the thermo-electro-magnetic-mechanical loadings along with various end supports, the GDQ method [46] is first used to discretize the nonlinear coupled equilibrium equations and associated boundary conditions. Then, the discretized equations are solved on the basis of the pseudo arc-length continuation method.

If N is the number of grid points in the x-direction, the grid points, ξ_i, on the basis of the shifted Chebyshev-Gauss-Lobatto grid points can be considered as:

$$\xi_i = \frac{1}{2}\left(1-\cos\frac{i-1}{N-1}\pi\right), \qquad i = 1, 2, \cdots, N. \quad (28)$$

Therefore, the discretized forms of the field variables u, w, θ_x, Φ, and ψ can be respectively expressed as column vectors $\mathbf{U}$, $\mathbf{W}$, $\boldsymbol{\theta}$, $\boldsymbol{\Phi}$, and $\boldsymbol{\Psi}$ defined as follows:

$$\mathbf{U} = \begin{bmatrix} u_1 & u_2 & \cdots & u_N \end{bmatrix}^T,$$
$$\mathbf{W} = \begin{bmatrix} w_1 & w_2 & \cdots & w_N \end{bmatrix}^T,$$
$$\boldsymbol{\theta} = \begin{bmatrix} \theta_{x1} & \theta_{x2} & \cdots & \theta_{xN} \end{bmatrix}^T,$$
$$\boldsymbol{\Phi} = \begin{bmatrix} \phi_1 & \phi_2 & \cdots & \phi_N \end{bmatrix}^T,$$
$$\boldsymbol{\Psi} = \begin{bmatrix} \psi_1 & \psi_2 & \cdots & \psi_N \end{bmatrix}^T, \quad (29)$$

in which $u_i = u(\xi_i)$, $w_i = w(\xi_i)$, $\theta_{xi} = \theta_x(\xi_i)$, $\phi_i = \phi(\xi_i)$, and $\psi_1 = \psi(\xi_i)$.

Moreover, on the basis of the GDQ method, the rth derivative of a continues function, $f(\xi)$, with respect to ξ can be approximately expressed as a linear sum of the function values as:

$$\frac{d^r f(\xi)}{d\xi^r} = \sum_{j=1}^{N} D_{ij}^{(r)} f(\xi_j) = \mathbf{D}_{\xi}^{(r)}\mathbf{F}, \quad (30)$$

where $[\mathbf{D}_{\xi}^{(r)}]_{ij} = D_{ij}^{(r)}$ denotes the weighting coefficients associated with the rth-order derivative expressed in the form of a recursion formula as:

$$\left[\mathbf{D}_{\xi}^{(r)}\right]_{ij} = \mathcal{W}_{ij}^{(r)} = \begin{cases} \mathbf{I}_x, & r = 0 \\ \frac{\mathcal{P}(\xi_i)}{(\xi_i - \xi_j)\mathcal{P}(\xi_j)}, & i \neq j \quad \text{and} \quad i, j = 1, \cdots, N \\ & \text{and} \quad r = 1 \\ r\left[\mathcal{W}_{ij}^{(1)}\mathcal{W}_{ii}^{(r-1)} - \frac{\mathcal{W}_{ij}^{(r-1)}}{\xi_i - \xi_j}\right], & i \neq j \quad \text{and} \quad i, j = 1, \cdots, N \\ & \text{and} \quad r = 2, 3, \cdots N-1 \\ -\sum_{j=1; j\neq i}^{N} \mathcal{W}_{ij}^{(r)}, & i = j \quad \text{and} \quad i, j = 1, \cdots, N \\ & \text{and} \quad r = 1, 2, 3, \cdots N-1 \end{cases} \tag{31}$$

where $\mathbf{I}_x$ denotes an $N \times N$ identity matrix and $\mathcal{P}(x_i) = \prod_{j=1; j\neq i}^{N} (\xi_i - \xi_j)$.

In the case of post-buckling problem, the applied external axial load is assumed to be $\bar{N}_x^0 = -p$. Transforming the equilibrium equations (Eqs. (22a)-(22e)) into the discrete forms according to the GDQ methods gives:

$$\mathbf{K}\mathbf{X} - p\mathbf{K}_{\mathbf{g}}\mathbf{X} + \mathbf{N}(\mathbf{X}) = \mathbf{0}, \tag{32}$$

where $\mathbf{X}$, $\mathbf{K}$, $\mathbf{K}_{\mathbf{g}}$, and $\mathbf{N}(\mathbf{X})$ are the field variables vector, stiffness matrix, geometric stiffness matrix, and nonlinear part vector, respectively, which are calculated by Eqs. (33a) to (33c) as shown in Box I. where $N = (\bar{N}_T + \bar{N}_E + \bar{N}_H)(\mathbf{D}_{\xi}^{(2)} - \epsilon^2 \mathbf{D}_{\xi}^{(4)})$. Moreover, the components of $\mathbf{N}(\mathbf{X})$ are defined in the following forms:

$$\mathbf{N}_u(\mathbf{X}) = \frac{\bar{A}_{11}}{\eta}\left(\mathbf{D}_{\xi}^{(1)}\mathbf{W}\right) \circ \left(\mathbf{D}_{\xi}^{(2)}\mathbf{W}\right), \tag{34a}$$

$$\mathbf{N}_w(\mathbf{X}) = \frac{\bar{A}_{11}}{\eta}\Bigg(\left(\mathbf{D}_{\xi}^{(1)}\mathbf{U}\right) \circ \left(\mathbf{D}_{\xi}^{(2)}\mathbf{W}\right) + \left(\mathbf{D}_{\xi}^{(2)}\mathbf{U}\right) \circ \left(\mathbf{D}_{\xi}^{(3)}\mathbf{W}\right) + \frac{3}{2\eta}\left(\mathbf{D}_{\xi}^{(2)}\mathbf{W}\right) \circ \left(\mathbf{D}_{\xi}^{(1)}\mathbf{W}\right) \circ \left(\mathbf{D}_{\xi}^{(1)}\mathbf{W}\right)\Bigg) - \epsilon^2\Bigg\{\frac{\bar{A}_{11}}{\eta}\Big(\left(\mathbf{D}_{\xi}^{(4)}\mathbf{U}\right) \circ \left(\mathbf{D}_{\xi}^{(1)}\mathbf{W}\right) + 3\left(\mathbf{D}_{\xi}^{(3)}\mathbf{U}\right) \circ \left(\mathbf{D}_{\xi}^{(2)}\mathbf{W}\right) + 3\left(\mathbf{D}_{\xi}^{(2)}\mathbf{U}\right) \circ \left(\mathbf{D}_{\xi}^{(3)}\mathbf{W}\right)\Big) + \frac{\bar{A}_{11}}{\eta}\left(\left(\mathbf{D}_{\xi}^{(1)}\mathbf{U}\right) \circ \left(\mathbf{D}_{\xi}^{(4)}\mathbf{W}\right)\right)$$

$$\mathbf{X} = \left[\mathbf{U}^T \quad \mathbf{W}^T \quad \boldsymbol{\theta}^T \quad \boldsymbol{\Phi}^T \quad \boldsymbol{\Psi}^T\right]^T, \tag{33a}$$

$$\mathbf{K} = \begin{bmatrix} \bar{A}_{11}\mathbf{D}_{\xi}^{(2)} & \mathbf{0} & \mathbf{0} & \mathbf{0} & \mathbf{0} \\ \mathbf{0} & k_s\bar{A}_{44}\mathbf{D}_{\xi}^{(2)} + N & k_s\bar{A}_{44}\eta\mathbf{D}_{\xi}^{(1)} & -k_s\bar{E}_{15}\mathbf{D}_{\xi}^{(2)} & -k_s\bar{Q}_{15}\mathbf{D}_{\xi}^{(2)} \\ \mathbf{0} & -k_s\bar{A}_{44}\eta\mathbf{D}_{\xi}^{(1)} & -k_s\bar{A}_{44}\eta^2\mathbf{D}_{\xi}^{(0)} + \bar{D}_{11}\mathbf{D}_{\xi}^{(2)} & \eta(\bar{E}_{31} + \kappa_s\bar{E}_{15})\mathbf{D}_{\xi}^{(1)} & \eta(\bar{Q}_{31} + \kappa_s\bar{Q}_{15})\mathbf{D}_{\xi}^{(1)} \\ \mathbf{0} & \bar{E}_{15}\mathbf{D}_{\xi}^{(2)} & (\bar{E}_{31} + \bar{E}_{15})\eta\mathbf{D}_{\xi}^{(1)} & -\bar{X}_{33}\eta^2\mathbf{D}_{\xi}^{(0)} + \bar{X}_{11}\mathbf{D}_{\xi}^{(2)} & -\bar{Y}_{33}\eta^2\mathbf{D}_{\xi}^{(0)} + \bar{Y}_{11}\mathbf{D}_{\xi}^{(2)} \\ \mathbf{0} & \bar{Q}_{15}\mathbf{D}_{\xi}^{(2)} & (\bar{Q}_{31} + \bar{Q}_{15})\eta\mathbf{D}_{\xi}^{(1)} & -\bar{Y}_{33}\eta^2\mathbf{D}_{\xi}^{(0)} + \bar{Y}_{11}\mathbf{D}_{\xi}^{(2)} & -\bar{T}_{33}\eta^2\mathbf{D}_{\xi}^{(0)} + \bar{T}_{11}\mathbf{D}_{\xi}^{(2)} \end{bmatrix}, \tag{33b}$$

$$\mathbf{K}_{\mathbf{g}} = \begin{bmatrix} \mathbf{0} & \mathbf{0} & \mathbf{0} & \mathbf{0} & \mathbf{0} \\ \mathbf{0} & \mathbf{D}_{\xi}^{(2)} - \epsilon^2\mathbf{D}_{\xi}^{(4)} & \mathbf{0} & \mathbf{0} & \mathbf{0} \\ \mathbf{0} & \mathbf{0} & \mathbf{0} & \mathbf{0} & \mathbf{0} \\ \mathbf{0} & \mathbf{0} & \mathbf{0} & \mathbf{0} & \mathbf{0} \\ \mathbf{0} & \mathbf{0} & \mathbf{0} & \mathbf{0} & \mathbf{0} \end{bmatrix}, \tag{33c}$$

$$\mathbf{N}(\mathbf{X}) = \left[\mathbf{N}_u^T(\mathbf{X}) \quad \mathbf{N}_w^T(\mathbf{X}) \quad \mathbf{N}_{\theta}^T(\mathbf{X}) \quad \mathbf{N}_{\phi}^T(\mathbf{X}) \quad \mathbf{N}_{\psi}^T(\mathbf{X})\right]^T. \tag{33e}$$

Box I

$$+\frac{\bar{A}_{11}}{\eta^2}\left(3\left(\mathbf{D}_\xi^{(2)}\mathbf{W}\right)\circ\left(\mathbf{D}_\xi^{(2)}\mathbf{W}\right)\circ\left(\mathbf{D}_\xi^{(2)}\mathbf{W}\right)\right)$$

$$+\frac{\bar{A}_{11}}{\eta^2}\left(9\left(\mathbf{D}_\xi^{(1)}\mathbf{W}\right)\circ\left(\mathbf{D}_\xi^{(2)}\mathbf{W}\right)\circ\left(\mathbf{D}_\xi^{(3)}\mathbf{W}\right)\right.$$

$$\left.+\frac{3}{2}\left(\mathbf{D}_\xi^{(1)}\mathbf{W}\right)\circ\left(\mathbf{D}_\xi^{(1)}\mathbf{W}\right)\circ\left(\mathbf{D}_\xi^{(4)}\mathbf{W}\right)\right)\Bigg\}, \quad (34b)$$

$$\mathbf{N}_\theta(\mathbf{X})=\mathbf{N}_\phi(\mathbf{X})=\mathbf{N}_\psi(\mathbf{X})=0, \quad (34c)$$

where $\circ$ is the Hadamard product defined in the Appendix. The boundary conditions can be discretized in the same way. For instance, the discretized edge conditions for an METE nanobeam with C-C end support (see Eq. (24)) can be written as:

$$\mathbf{U}=\mathbf{W}=\boldsymbol{\theta}=\boldsymbol{\Phi}=\boldsymbol{\psi}=0 \qquad \text{at} \qquad \xi=0,1. \quad (35)$$

The governing equations of the domain equilibrium together with associated edge conditions represent a set of nonlinear problems of the form:

$$\mathbf{F}:\ \mathbb{R}^{5N+1}\rightarrow\mathbb{R}^{5N}, \quad \mathbf{F}(p,\mathbf{X})=0. \quad (36)$$

The pseudo arc-length continuation algorithm [47] is utilized to estimate the post-buckling path of METE nanobeams under the magneto-electro-thermo-mechanical loading.

5. Results and discussion

In this section, numerical results are provided to examine the size-dependent post-buckling behavior of the METE nanobeams with SS-SS, C-SS, and C-C end supports subjected to magneto-electro-thermo-mechanical loading. It is assumed that the METE nanobeams are made of the two-phase $BiTiO_3$-$CoFe_2O_4$ composites with the material properties given in Table 1 [36,48-50]. The influences of the non-dimensional nonlocal parameter, external magnetic potential, external electric potential, and temperature rise on the post-buckling path of the METE nanobeams are discussed in detail.

First of all, in order to verify validity of the proposed model and solution methodology, the first three normalized critical buckling loads ($\tilde{P}=N_x^0L^2/12D_{11}$) of METE nanobeam with SS-SS edge supports corresponding to various nonlocal parameters are listed in Table 2 and compared with the analytical results given by Li et al. [51]. It can be found that the results provided in this investigation are in good agreement with those of Li et al. [51].

The influence of the non-dimensional nonlocal parameter, μ, on the post-buckling path of METE nanobeams with SS-SS, C-SS, and C-C edge supports corresponding to the first and second buckling modes, respectively, is represented in Figures 2 and 3, where the non-dimensional maximum deflection of the METE nanobeam ($w_{\max}$) versus the non-dimensional applied compressive axial load is plotted. The non-dimensional applied compressive axial load is defined as $P=N_x^0L^2/D_{11}$. Moreover, in addition to the associated critical buckling loads, the results of the classical METE beam ($\mu=0$) are given for a direct comparison. For all types of edge supports, an increase in the non-dimensional nonlocal parameter decreases

Table 1. Material properties of $BiTiO_3$-$CoFe_2O_4$ composite materials.

Properties	$BiTiO_3$-$CoFe_2O_4$
Elastic (GPa)	$c_{11}=226$; $c_{12}=125$; $c_{13}=124$; $c_{33}=216$; $c_{44}=44.2$
Piezoelectric (C/m^2)	$e_{31}=2.2$; $e_{33}=9.3$; $e_{15}=5.8$
Dielectric (10^9 C/V.m)	$s_{11}=5.64$; $s_{33}=6.35$
Piezomagnetic (N/A.m)	$q_{15}=275$; $q_{31}=290.1$; $q_{33}=349.9$
Magnetoelectric (10^{12} Ns/VC)	$d_{11}=5.367$; $d_{33}=2737.5$
Magnetic (10^6 Ns^2/C^2)	$\mu_{11}=-297$; $\mu_{33}=83.5$
Thermal moduli (10^5 N/K.m^2)	$\beta_1=4.74$; $\beta_3=4.53$
Pyroelectric (10^6 C/N)	$p_3=25$
Pyromagnetic (10^6 N/A.m.K)	$\lambda_3=5.19$

Table 2. Normalized buckling loads ($\tilde{P}=N_x^0L^2/12D_{11}$) of METE nanobeam with SS-SS edge conditions ($L=10$ nm, $h=0.4$ nm, and $V_E=\Omega_H=\Delta T=0$).

Mode	$e_0a=0$ nm		$e_0a=1$ nm		$e_0a=2$ nm		$e_0a=3$ nm	
	Ref. [51]	Present	Ref. [51]	Present	Ref. [51]	Present	Ref. [51]	Present
1	0.8189	0.8192	0.7198	0.7204	0.5564	0.5595	0.4089	0.4114
2	3.1595	3.1620	2.0462	2.0529	1.1026	1.1096	0.6365	0.6384
3	6.7046	6.7563	3.0463	3.0540	1.3102	1.3137	0.6877	0.6936

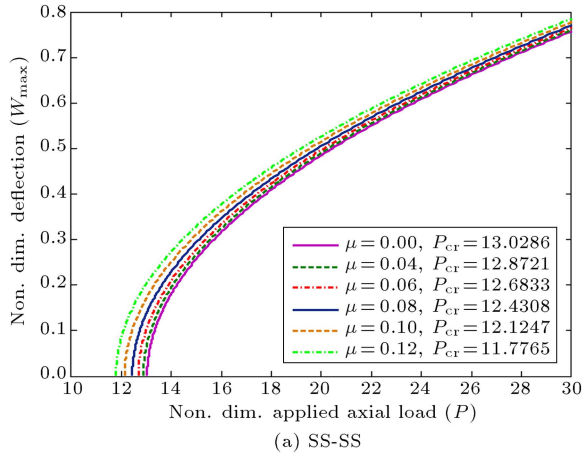

(a) SS-SS

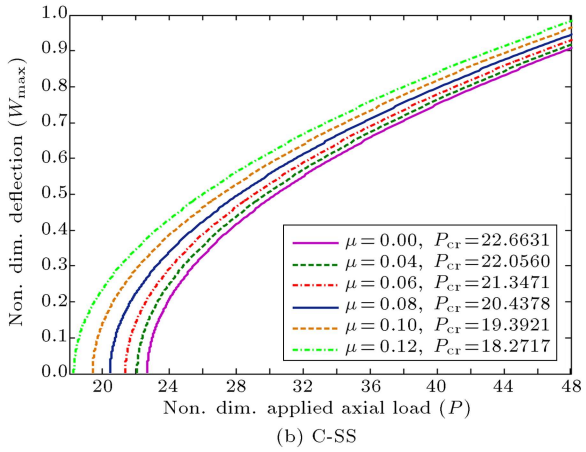

(b) C-SS

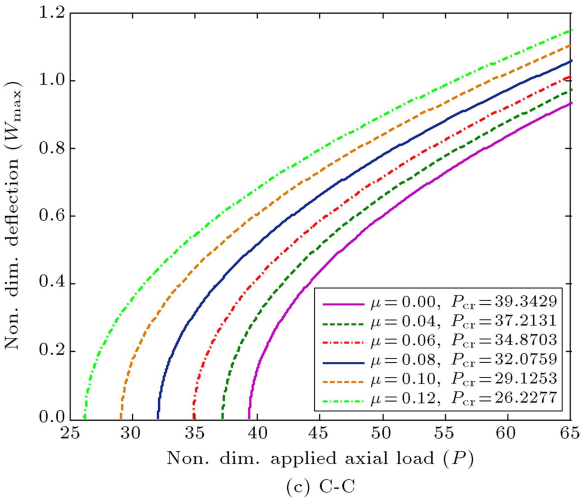

(c) C-C

Figure 2. Post-buckling path of METE nanobeams associated with different nonlocal parameters and boundary conditions corresponding to the first mode ($L/h = 10$, $h = 10$ nm, $V_E = -0.02$ V, $\Omega_H = 0.02$ A, and $\Delta T = 20^{\circ}$C).

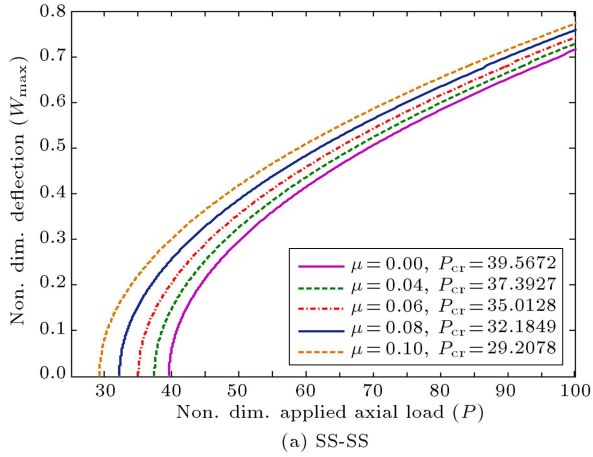

(a) SS-SS

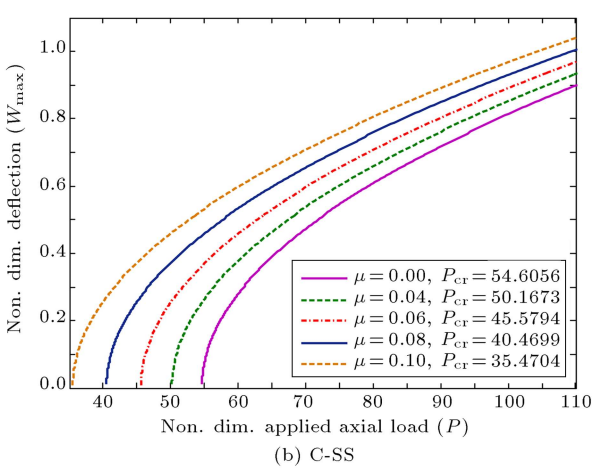

(b) C-SS

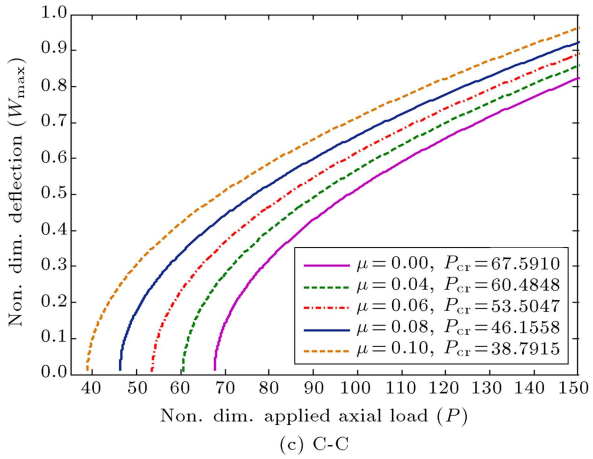

(c) C-C

Figure 3. Post-buckling path of METE nanobeams associated with different nonlocal parameters and boundary conditions corresponding to the second mode ($L/h = 10$, $h = 10$ nm, $V_E = -0.02$ V, $\Omega_H = 0.02$ A, and $\Delta T = 20^{\circ}$C).

the critical buckling load and for a given applied load in the post-buckling domain, the maximum deflection of METE nanobeam increases. The reason is that the nonlocal METE nanobeam model predicts the lower stiffness values compared to the classical beam model. Moreover, compared to the METE nanobeams with C-SS and C-C end conditions, the nonlocal parameter has lesser influence on the critical buckling load and post-buckling path of SS-SS METE nanobeams. Another finding is that the effect of nonlocal parameter on the critical buckling load and post-buckling path of METE

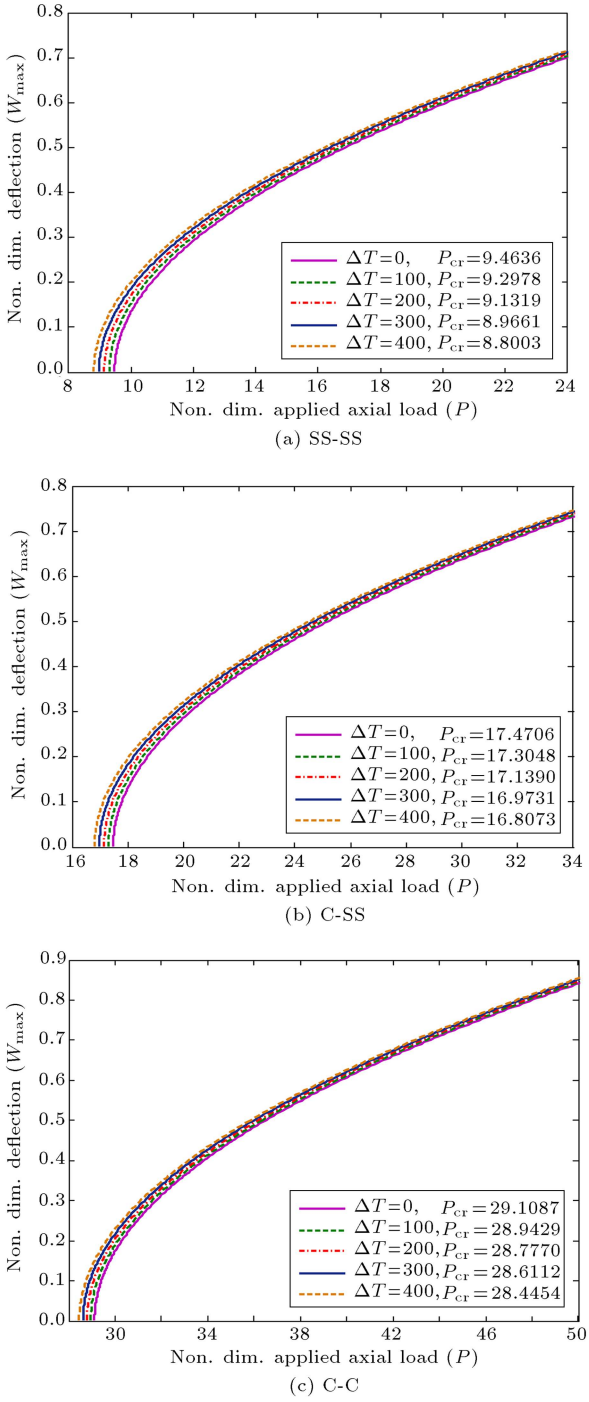

Figure 4. Post-buckling path of METE nanobeams associated with different temperature changes and boundary conditions ($L/h = 10$, $h = 10$ nm, $V_E = 0$ V, $\Omega_H = 0$ A, and $\mu = 0.08$).

nanobeam associated with the second mode is more significant than in the first buckling mode.

Figure 4 shows the effect of temperature rise on the critical buckling load and post-buckling path of METE nanobeams with SS-SS, C-SS, and C-C boundary conditions. According to this figure, with increasing the temperature change, the critical buckling load decreases and maximum deflection of METE nanobeam in the post-buckling domain increases. In fact, increasing the temperature rise generates higher axial compressive loads, leading to more reduction in the stiffness of METE nanobeams. Moreover, it can be seen that the influence of temperature rise for METE nanobeams with SS-SS edge conditions is more considerable than that for other ones.

The effect of external electric voltage on the post-buckling responses of METE nanobeams with SS-SS, C-SS, and C-SS edge conditions is examined in Figure 5. It can be seen that, due to the imposed positive electric voltages, the METE nanobeam experiences larger post-buckling deformations than in the cases without and with negative electric voltages. Moreover, the positive values of external electric voltage decrease the critical buckling load of METE nanobeams, while the negative electric voltages have an increasing effect. In fact, the positive and negative external electric voltages respectively generate compressive and tensile in-plane forces in the METE nanobeams leading to decrease and increase in the stiffness of nanobeams, correspondingly.

Figure 6 depicts the post-buckling responses of METE nanobeams subjected to various external magnetic potentials. The METE nanobeams subjected to the negative external magnetic potentials undergo larger post-buckling deformations and lower critical buckling loads, indicating that higher negative magnetic potentials cause the stability of METE nanobeams to decrease. The reason is that negative magnetic potentials generate a compressive axial force and, consequently, lead to decrease in the stiffness of METE nanobeams. Obviously, the positive external magnetic potentials can lead to high critical buckling loads and a considerable increase in the post-buckling load-carrying capacity in comparison with the negative magnetic potentials.

6. Concluding remarks

In the present study, the size-dependent post-buckling characteristics of METE nanobeams subjected to the magneto-electro-thermo-mechanical loading were examined. To this end, a size-dependent nonlinear first-order shear deformable nanobeam model was developed, which contained the effects of small-scale parameter, thermo-electro-magnetic-mechanical loading, and transverse shear deformation. Using the Eringen's nonlocal elasticity theory, first-order shear deformation beam theory, and von Kármán hypothesis, the nonlinear governing equations and corresponding boundary conditions were obtained. The GDQ method was used to discretize the nonlinear governing equations, which were then solved using the pseudo arc-length continuation method to obtain the post-buckling path

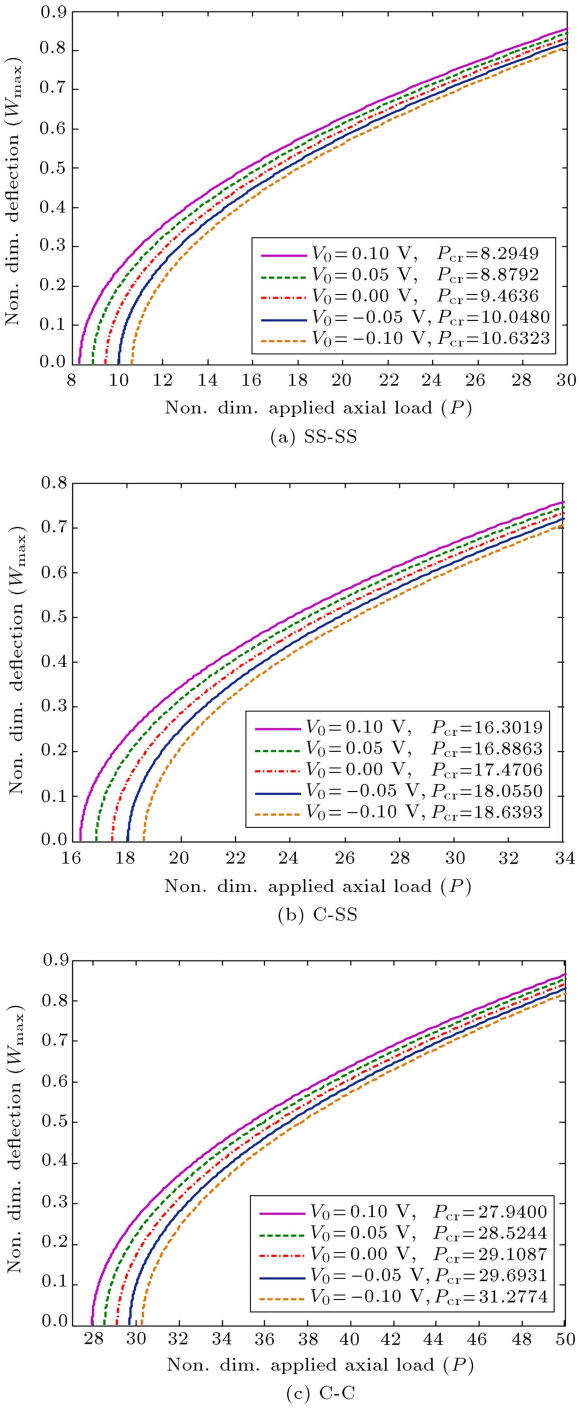

Figure 5. Post-buckling path of METE nanobeams associated with different external electric voltages and boundary conditions ($L/h = 10$, $h = 10$ nm, $\Omega_H = 0$ A, $\Delta T = 0^\circ$C, and $\mu = 0.08$).

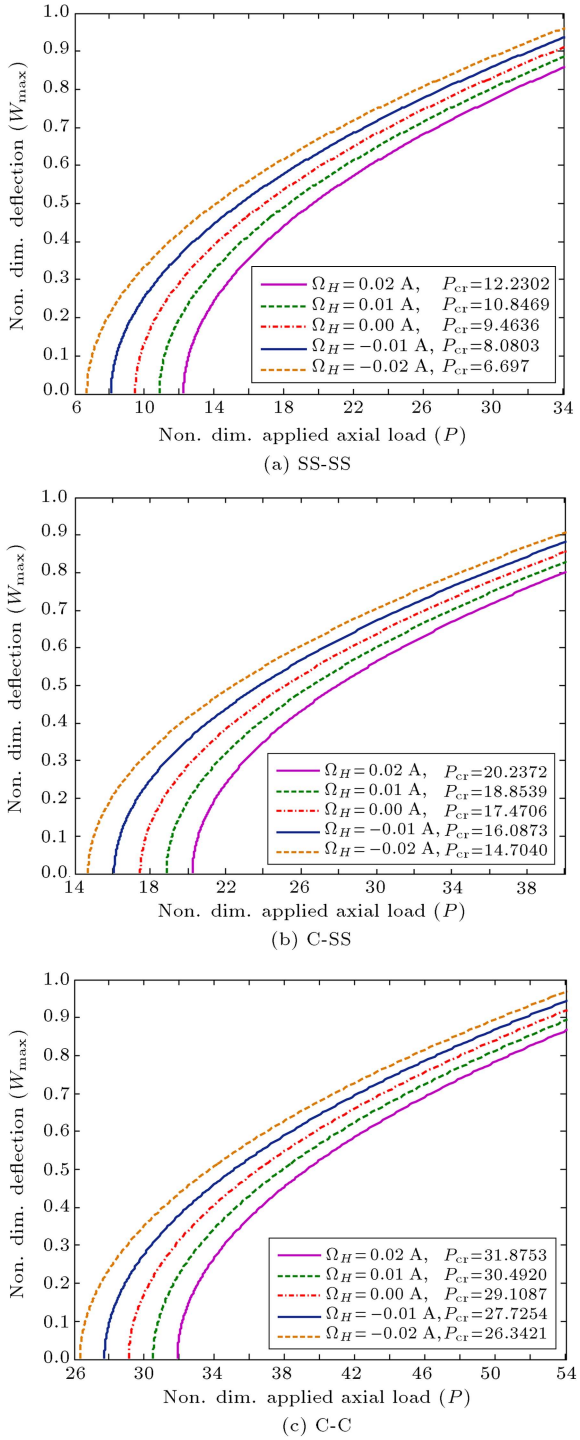

Figure 6. Post-buckling path of METE nanobeams associated with different external magnetic potentials and boundary conditions ($L/h = 10$, $h = 10$ nm, $V_E = 0$ V, $\Delta T = 0^\circ$C, and $\mu = 0.08$).

of the METE nanobeams under various edge supports. Finally, the effects of various parameters such as nonlocal parameter, external electric voltage, external magnetic potential, and temperature rise on the post-buckling path of METE nanobeams were examined in detail. The results revealed that an increase in the non-dimensional nonlocal parameter as well as temperature rise decreased the critical buckling load and post-buckling load-carrying capacity of METE nanobeams. Moreover, due to the imposed negative electric voltages and positive magnetic potentials, the critical buckling load as well as post-buckling strength of the METE nanobeams increased.

References

1. Van den Boomgaard, J., Terrell, D., Born, R. and Giller, H. "An in situ grown eutectic magnetoelectric composite material", *Journal of Materials Science*, **9**, pp. 1705-1709 (1974).
2. Lang, Z. and Xuewu, L. "Buckling and vibration analysis of functionally graded magneto-electro-thermo-elastic circular cylindrical shells", *Applied Mathematical Modelling*, **37**, pp. 2279-2292 (2013).
3. Brischetto, S. and Carrera, E. "Coupled thermo-electro-mechanical analysis of smart plates embedding composite and piezoelectric layers", *Journal of Thermal Stresses*, **35**, pp. 766-804 (2012).
4. Ballato, A. "Modeling piezoelectric and piezomagnetic devices and structures via equivalent networks", *IEEE Transactions on Ultrasonics, Ferroelectrics, and Frequency Control*, **48**, pp. 1189-1240 (2001).
5. Zhang, C., Chen, W., Li, J. and Yang, J. "One-dimensional equations for piezoelectromagnetic beams and magnetoelectric effects in fibers", *Smart Materials and Structures*, **18**, 095026 (2009).
6. Newnham, R.E., Bowen, L., Klicker, K. and Cross, L. "Composite piezoelectric transducers", *Materials & Design*, **2**, pp. 93-106 (1980).
7. Bailey, T. and Ubbard, J. "Distributed piezoelectric-polymer active vibration control of a cantilever beam", *Journal of Guidance, Control, and Dynamics*, **8**, pp. 605-611 (1985).
8. Crawley, E.F. and De Luis, J. "Use of piezoelectric actuators as elements of intelligent structures", *AIAA Journal*, **25**, pp. 1373-1385 (1987).
9. Azvine, B., Tomlinson, G. and Wynne, R. "Use of active constrained-layer damping for controlling resonant vibration", *Smart Materials and Structures*, **4**, p. 1 (1995).
10. Baz, A. "Robust control of active constrained layer damping", *Journal of Sound and Vibration*, **211**, pp. 467-480 (1998).
11. Jiang, A.Q., Wang, C., Jin, K.J., et al. "A resistive memory in semiconducting $BiFeO_3$ thin-film capacitors", *Advanced Materials*, **23**, pp. 1277-1281 (2011).
12. Wang, Y., Hu, J., Lin, Y. and Nan, C.-W. "Multiferroic magnetoelectric composite nanostructures", *NPG Asia Materials*, **2**, pp. 61-68 (2010).
13. Béa, H., Gajek, M., Bibes, M. and Barthélémy, A. "Spintronics with multiferroics", *Journal of Physics: Condensed Matter*, **20**, p. 434221 (2008).
14. Chu, Y., Zhao, T., Cruz, M., et al. "Ferroelectric size effects in multiferroic BiFeO3 thin films", *Applied Physics Letters*, **90**, p. 252906 (2007).
15. Ren, W. and Bellaiche, L. "Size effects in multiferroic $BiFeO_3$ nanodots: a first-principles-based study", *Physical Review B*, **82**, p. 113403 (2010).
16. Miller, R.E. and Shenoy, V.B. "Size-dependent elastic properties of nanosized structural elements", *Nanotechnology*, **11**, p. 139 (2000).
17. Xu, F., Qin, Q., Mishra, A., Gu, Y. and Zhu, Y. "Mechanical properties of ZnO nanowires under different loading modes", *Nano Research*, **3**, pp. 271-280 (2010).
18. Ansari, R., Oskouie, M.F. and Gholami, R. "Size-dependent geometrically nonlinear free vibration analysis of fractional viscoelastic nanobeams based on the nonlocal elasticity theory", *Physica E: Low-dimensional Systems and Nanostructures*, **75**, pp. 266-271 (2015).
19. Ansari, R., Gholami, R., Sahmani, S., Norouzzadeh, A. and Bazdid-Vahdati, M. "Dynamic stability analysis of embedded multi-walled carbon nanotubes in thermal environment", *Acta Mechanica Solida Sinica*, **28**, pp. 659-667 (2015).
20. Ansari, R. and Gholami, R. "Dynamic stability of embedded single-walled carbon nanotubes including thermal effects", *Iranian Journal of Science and Technology Transactions of Mechanical Engineering*, **39**, pp. 153-161 (2015).
21. Wang, C., Zhang, J., Fei, Y. and Murmu, T. "Circumferential nonlocal effect on vibrating nanotubules", *International Journal of Mechanical Sciences*, **58**, pp. 86-90 (2012).
22. Gholami, R., Darvizeh, A., Ansari, R. and Sadeghi, F. "Vibration and buckling of first-order shear deformable circular cylindrical micro-/nano-shells based on Mindlin's strain gradient elasticity theory", *European Journal of Mechanics-A/Solids*, **58**, pp. 76-88 (2016).
23. Yan, Y. and Wang, W. "Axisymmetric vibration of SWCNTs in water with arbitrary chirality based on nonlocal anisotropic shell model", *Applied Mathematical Modelling*, **39**, pp. 3016-3023 (2015).
24. Ansari, R., Gholami, R. and Sahmani, S. "On the dynamic stability of embedded single-walled carbon nanotubes including thermal environment effects", *Scientia Iranica*, **19**, pp. 919-925 (2012).
25. Wang, W., Li, P., Jin, F. and Wang, J. "Vibration analysis of piezoelectric ceramic circular nanoplates considering surface and nonlocal effects", *Composite Structures*, **140**, pp. 758-775 (2016).
26. Ansari, R. and Gholami, R. "Surface effect on the large amplitude periodic forced vibration of first-order shear deformable rectangular nanoplates with various edge supports", *Acta Astronautica*, **118**, pp. 72-89 (2016).
27. Ansari, R., Norouzzadeh, A., Gholami, R., Shojaei, M.F. and Darabi, M. "Geometrically nonlinear free vibration and instability of fluid-conveying nanoscale pipes including surface stress effects", *Microfluidics and Nanofluidics*, **20**, pp. 1-14 (2016).
28. Eringen, A.C. "Nonlocal polar elastic continua", *International Journal of Engineering Science*, **10**, pp. 1-16 (1972).
29. Eringen, A.C. "On differential equations of nonlocal elasticity and solutions of screw dislocation and surface waves", *Journal of Applied Physics*, **54**, pp. 4703-4710 (1983).

30. Eringen, A.C., *Nonlocal Continuum Field Theories: Springer Science & Business Media* (2002).

31. Asemi, S., Farajpour, A. and Mohammadi, M. "Nonlinear vibration analysis of piezoelectric nanoelectromechanical resonators based on nonlocal elasticity theory", *Composite Structures*, **116**, pp. 703-712 (2014).

32. Liu, C., Ke, L.-L., Wang, Y.-S., Yang, J. and Kitipornchai, S. "Thermo-electro-mechanical vibration of piezoelectric nanoplates based on the nonlocal theory", *Composite Structures*, **106**, pp. 167-174 (2013).

33. Ke, L.-L., Wang, Y.-S. and Wang, Z.-D. "Nonlinear vibration of the piezoelectric nanobeams based on the nonlocal theory", *Composite Structures*, **94**, pp. 2038-2047 (2012).

34. Ansari, R., Oskouie, M.F., Gholami, R. and Sadeghi, F. "Thermo-electro-mechanical vibration of postbuckled piezoelectric Timoshenko nanobeams based on the nonlocal elasticity theory", *Composites Part B: Engineering*, **89**, pp. 316-327 (2016).

35. Ke, L.-L. and Wang, Y.-S. "Thermoelectric-mechanical vibration of piezoelectric nanobeams based on the nonlocal theory", *Smart Materials and Structures*, **21**, p. 025018 (2012).

36. Ke, L.-L. and Wang, Y.-S. "Free vibration of size-dependent magneto-electro-elastic nanobeams based on the nonlocal theory", *Physica E: Low-dimensional Systems and Nanostructures*, **63**, pp. 52-61 (2014).

37. Ke, L.-L., Wang, Y.-S., Yang, J. and Kitipornchai, S. "Free vibration of size-dependent magneto-electro-elastic nanoplates based on the nonlocal theory", *Acta Mechanica Sinica*, **30**, pp. 516-525 (2014).

38. Ke, L.-L., Liu, C. and Wang, Y.-S. "Free vibration of nonlocal piezoelectric nanoplates under various boundary conditions", *Physica E: Low-dimensional Systems and Nanostructures*, **66**, pp. 93-106 (2015).

39. Li, Y., Cai, Z. and Shi, S. "Buckling and free vibration of magnetoelectroelastic nanoplate based on nonlocal theory", *Composite Structures*, **111**, pp. 522-529 (2014).

40. Ke, L.-L., Wang, Y.-S., Yang, J. and Kitipornchai, S. "The size-dependent vibration of embedded magneto-electro-elastic cylindrical nanoshells", *Smart Materials and Structures*, **23**, p. 125036 (2014).

41. Liang, X., Hu, S. and Shen, S. "Surface effects on the post-buckling of piezoelectric nanowires", *Physica E: Low-dimensional Systems and Nanostructures*, **69**, pp. 61-64 (2015).

42. Zhang, L., Liu, J., Fang, X. and Nie, G. "Effects of surface piezoelectricity and nonlocal scale on wave propagation in piezoelectric nanoplates", *European Journal of Mechanics-A/Solids*, **46**, pp. 22-29 (2014).

43. Gheshlaghi, B. and Hasheminejad, S.M. "Vibration analysis of piezoelectric nanowires with surface and small scale effects", *Current Applied Physics*, **12**, pp. 1096-1099 (2012).

44. Hosseini-Hashemi, S., Nahas, I., Fakher, M. and Nazemnezhad, R. "Surface effects on free vibration of piezoelectric functionally graded nanobeams using nonlocal elasticity", *Acta Mechanica*, **225**, pp. 1555-1564 (2014).

45. Zhang, C., Chen, W. and Zhang, C. "Two-dimensional theory of piezoelectric plates considering surface effect", *European Journal of Mechanics-A/Solids*, **41**, pp. 50-57 (2013).

46. Bellman, R., Kashef, B. and Casti, J. "Differential quadrature: a technique for the rapid solution of nonlinear partial differential equations", *Journal of Computational Physics*, **10**, pp. 40-52 (1972).

47. Keller, H.B. "Numerical solution of bifurcation and nonlinear eigenvalue problems", *Applications of Bifurcation Theory*, pp. 359-384 (1977).

48. Li, J.Y. "Magnetoelectroelastic multi-inclusion and inhomogeneity problems and their applications in composite materials", *International Journal of Engineering Science*, **38**, pp. 1993-2011 (2000).

49. Bin, W., Jiangong, Y. and Cunfu, H. "Wave propagation in non-homogeneous magneto-electro-elastic plates", *Journal of Sound and Vibration*, **317**, pp. 250-264 (2008).

50. Hou, P.-F., Teng, G.-H. and Chen, H.-R. "Three-dimensional Green's function for a point heat source in two-phase transversely isotropic magneto-electro-thermo-elastic material", *Mechanics of Materials*, **41**, pp. 329-338 (2009).

51. Li, Y., Ma, P. and Wang, W. "Bending, buckling, and free vibration of magnetoelectroelastic nanobeam based on nonlocal theory", *Journal of Intelligent Material Systems and Structures*, **27**(9), pp. 1139-1149 (2016).

Appendix

Hadamard Products: Let $\mathbf{A} = [A_{ij}]_{N\times M}$ and $\mathbf{B} = [B_{ij}]_{N\times M}$; then, the Hadamard product of these matrices can be expressed as $\mathbf{A} \circ \mathbf{B} = [A_{ij}B_{ij}]_{N\times M}$.

Biographies

Reza Ansari received his PhD degree from University of Guilan, Iran, in 2008, where he is currently a faculty member in the Department of Mechanical Engineering. During his PhD program. He was also a visiting fellow at Wollongong University, Australia, from 2006 to 2007. He has authored more than 200 refereed journal papers and 12 book chapters. His research background and interests include computational mechanics; numerical analysis; continuum mechanics; and nano-, micro-, and macro-mechanics.

Raheb Gholami received his BS, MS, and PhD degrees in Mechanical Engineering from University of

Guilan, Iran, in 2008, 2010, and 2015, respectively. He is currently a faculty member in the Department of Mechanical Engineering, Lahijan Branch, Islamic Azad University. His research background and interests include computational micro- and nano-mechanics; numerical techniques; nonlinear analyses; and prediction of mechanical behavior of beam, plate, and shell-type structures.